

Blockade of pan-viral propagation by inhibition of host cell PNPT1

Shuang Qu^{a,†}, Chen Yang^{b,†}, Xinlei Sun^{a,†}, Hai Huang^{b,†}, Jiacheng Li^b, Yujie Zhu^b,
Yaliang Zhang^b, Limin Li^a, Hongwei Liang^{a,*}, Ke Zen^{b,*}

^a School of Life Science and Technology, China Pharmaceutical University, Nanjing, Jiangsu, China

^b Department of Gastroenterology, Drum Tower Hospital, State Key Laboratory of Pharmaceutical Biotechnology, Nanjing University Medical School, Nanjing, Jiangsu, China

ARTICLE INFO

Article history:

Received 15 June 2023

Accepted 21 February 2024

Editor: Professor Philippe Colson

Keywords:

PNPT1

mt-dsRNAs

Lanatoside C

Pan-viral replication

ISR

SARS-CoV-2

ABSTRACT

For successful viral propagation within infected cells, the virus needs to overcome the cellular integrated stress response (ISR), triggered during viral infection, which, in turn, inhibits general protein translation. This paper reports a tactic employed by viruses to suppress the ISR by upregulating host cell polyribonucleotide nucleotidyltransferase 1 (PNPT1). The propagation of adenovirus, murine cytomegalovirus and hepatitis virus within their respective host cells induces PNPT1 expression. Notably, when PNPT1 is knocked down, the propagation of all three viruses is prevented. Mechanistically, the inhibition of PNPT1 facilitates the relocation of mitochondrial double-stranded RNAs (mt-dsRNAs) to the cytoplasm, where they activate RNA-activated protein kinase (PKR). This activation leads to eukaryotic initiation factor 2 α (eIF2 α) phosphorylation, resulting in the suppression of translation. Furthermore, by scrutinizing the PNPT1 recognition element and screening 17,728 drugs and bioactive compounds approved by the US Food and Drug Administration, lanatoside C was identified as a potent PNPT1 inhibitor. This compound impedes the propagation of adenovirus, murine cytomegalovirus and hepatitis virus, and suppresses production of the severe acute respiratory syndrome coronavirus-2 spike protein. These discoveries shed light on a novel strategy to impede pan-viral propagation by activating the host cell mt-dsRNA-PKR-eIF2 α signalling axis.

© 2024 The Authors. Published by Elsevier Ltd.

This is an open access article under the CC BY-NC-ND license (<http://creativecommons.org/licenses/by-nc-nd/4.0/>)

1. Introduction

Viral infection, particularly the coronavirus disease 2019 (COVID-19) pandemic, has a significant effect on everyday life and presents a major challenge to human health. Viruses have developed various mechanisms to infect their respective host cells [1,2]. Regardless of how viruses enter their host cells, they need to hijack the protein translation machinery of the infected cells to produce viral proteins for successful propagation. Rapid viral replication likely exerts major stress on mitochondria within the host cells [3,4]. Mitochondrial gene transcription and production are markedly increased during viral infection [5,6]. In most eukaryotic cells, mitochondria serve as semiautonomous

organelles that play a pivotal role in not only the production of adenosine-5'-triphosphate (ATP) via oxidative phosphorylation, but also regulation of the antiviral innate immunity system. Through antiviral-signalling protein (MAVS) [7–9], mitochondria act as a platform to link various pattern recognition receptors that recognize viral RNAs and initiate a conserved antiviral programme. For instance, uncapped 5'-triphosphate double-stranded [10–12] and long dsRNA [13] can be recognized by RIG-I and MDA5 helicases, two major components of the MAVS-dependent pathway [13]. Mitochondria double-stranded RNAs (mt-dsRNAs), a potential major source of endogenous double-stranded RNAs (dsRNAs) in mammalian cells [14], also display immunogenic capacity to activate antiviral immune responses. Mitochondria gene transcription and production enhanced by viral infection likely promotes the generation of mt-dsRNAs in mitochondria [15]. Although the underlying mechanism remains incompletely understood, enhanced production of mt-dsRNAs in mitochondria likely leads to the leakage of mt-dsRNAs into cytoplasm, where they can be detected by different dsRNA sensors, including RNA-activated protein kinase (PKR) [16]. Activation of PKR by mt-dsRNAs may further phosphorylate eukaryotic initiation factor 2 α (eIF2 α), resulting in the termination

* Corresponding authors. Addresses: K. Zen, State Key Laboratory of Pharmaceutical Biotechnology, Nanjing University Medical School, Nanjing, Jiangsu 210093, China. H. Liang, School of Life Science and Technology, China Pharmaceutical University, Nanjing, Jiangsu 211198, China.

E-mail addresses: lianghongwei0418@163.com (H. Liang), kzen@nju.edu.cn (K. Zen).

[†] These authors contributed equally to this work

of general protein translation [17]. As phosphorylation of eIF2 α in the host cells can shut down general protein synthesis, which prevents viral replication and eventually leads to cell apoptosis, mt-dsRNA-activated PKR signalling serves as an important component of the mitochondria-based antiviral immune system [17].

For successful propagation, viruses need to develop sophisticated mechanisms to evade either MAVS-mediated antiviral immune responses or the PKR-eIF2 α axis-mediated integrated stress response (ISR). Although the molecular basis governing these processes remains incompletely understood, one possible mechanism is the activation of a specific endoribonuclease or nucleotidyltransferase to degrade the viral and endogenous dsRNA. For instance, Burke et al. [18] reported the critical role of RNase L in arresting nuclear mRNA export, which strongly inhibits influenza A virus protein synthesis and cytokine production. Polyribonucleotide nucleotidyltransferase 1 (PNPT1), a conserved polynucleotide phosphorylase with phosphate-dependent 3'-to-5' exoribonuclease activity [19], was strongly upregulated during viral infection. PNPT1, accompanied by SUV3, is responsible for RNA processing and degradation in mitochondria, and thus maintaining homeostasis of mitochondria RNA [19]. PNPT1 deficiency has been shown to cause significant relocation of mt-dsRNAs from mitochondria to cytoplasm [16]. Previous studies by different investigators reported that PNPT1 could be modulated by interferon (IFN) signals, particularly IFN α and IFN β [20,21], suggesting that viruses may be able to regulate the level of PNPT1 in the host cells as viral infection generally produces strong IFN signals.

Given that PNPT1 induced by replication of various viruses plays a critical role in controlling the leakage of dsRNAs from mitochondria to cytoplasm, it was postulated that the inhibition of PNPT1 would elicit the host cell ISR induced by mt-dsRNAs, and thus prevent pan-viral propagation. This study used three different viral infection systems, and demonstrated the induction of PNPT1 as a common strategy for viruses to suppress the ISR in infected cells. PNPT1 knockdown was found to prevent propagation of all three viruses tested in this study. Mechanistic studies have suggested that the inhibition of PNPT1 promotes the leakage of mt-dsRNAs into cytoplasm, and these cytosolic mt-dsRNAs bind to

PKR and activate PKR-eIF2 α signalling, leading to termination of the general translation process. Moreover, through analysing the element of PNPT1 recognition, and screening 17,728 drugs and bioactive compounds approved by the US Food and Drug Administration (FDA), this study identified lanatoside C (LanC) as a potent PNPT1 inhibitor. LanC blocks the propagation of adenovirus (Adv-5), murine cytomegalovirus (MCMV) and murine hepatovirus (MHV), as well as production of the severe acute respiratory syndrome coronavirus-2 (SARS-CoV-2) spike protein (S-protein), in respective host cells, supporting the hypothesis that pan-viral propagation in infected cells can be shut down by PNPT1 inhibition.

2. Results

2.1. Induction of host cell PNPT1 serves as a common strategy for viral replication

BEAS-2B, NIH-3T3 and Neuro-2a cells were infected with Adv-5, MCMV and MHV-A59, respectively, in order to monitor host cell PNPT1 levels during viral replication. Immunofluorescence labelling (Fig. 1a,c,e) showed that host cell PNPT1 levels were markedly increased following viral infection. Dose-dependent up-regulation of host cell PNPT1 during various viral infections was further confirmed by Western blot analysis (Fig. 1b,d,f). Viral-infection-mediated PNPT1 induction supported previous reports that viral-infection-associated IFN signals could promote PNPT1 expression [20,21].

Next, the role of PNPT1 in viral replication was tested by depleting host cell PNPT1 via PNPT1-specific shRNA. As shown in Fig. S1a (see online supplementary material), PNPT1 levels in BEAS-2B, NIH-3T3 and Neuro-2a cells were reduced significantly by PNPT1-shRNA (sh-PNPT1) compared with those treated with control shRNA (sh-CTL). Knockdown of PNPT1 by PNPT1-shRNA did not affect host cell viability (Fig. S1b). In line with this, knockdown of PNPT1 did not change the virus level in the host cell after 1 h of infection (Fig. S1c), suggesting that host cell PNPT1 is not involved in the virus entering the host cells. However, the knockdown of host cell PNPT1 decreased the intracellular levels of Adv-5, MCMV

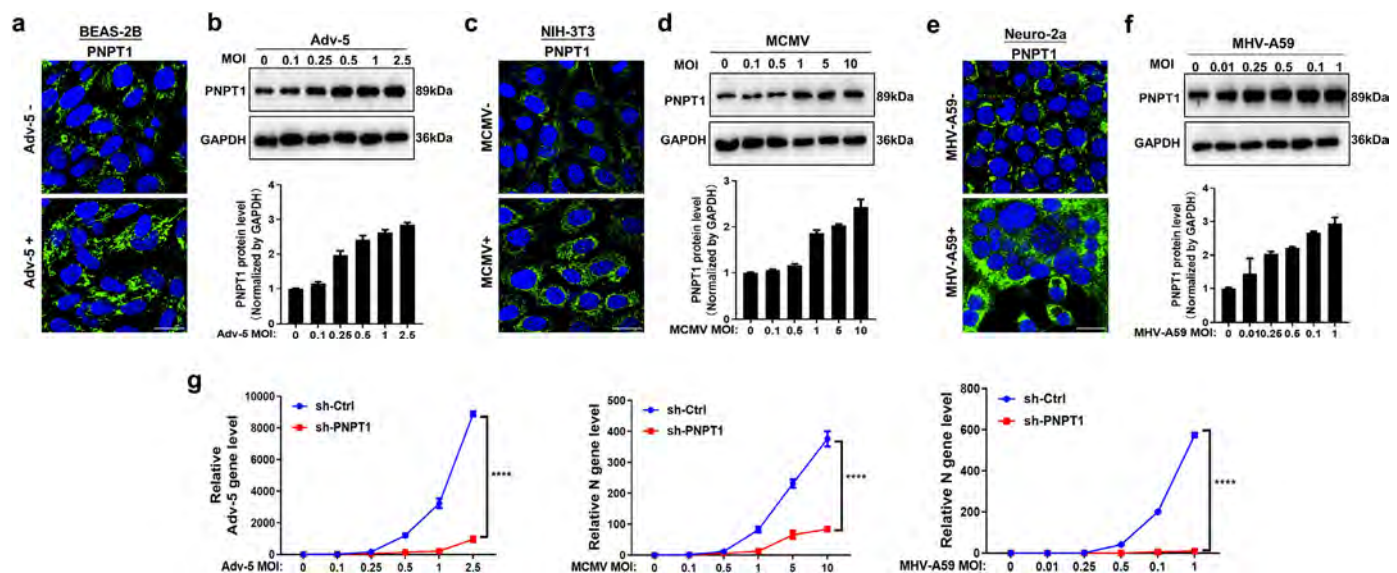


Fig. 1. Upregulation of polyribonucleotide nucleotidyltransferase 1 (PNPT1) in host cells infected by various viruses and depletion of PNPT1 in host cells markedly reduced viral replication. Immunostaining (a) and Western blot analysis (b) of PNPT1 in BEAS-2B cells with or without adenovirus (Adv-5) infection (24 h). Immunostaining (c) and Western blot analysis (d) of PNPT1 in NIH-3T3 cells with or without murine cytomegalovirus (MCMV) infection (48 h). Immunostaining (e) and Western blot analysis (f) of PNPT1 in Neuro-2a cells with or without murine hepatovirus (MHV-A59) infection (12 h). (g) Quantitative reverse transcription polymerase chain reaction analysis of viral DNA level in BEAS-2B cells (left), NIH-3T3 cells (middle) and Neuro-2a cells (right) with or without Adv-5, MCMV or MHV-A59 infection for 12 h, 24 h or 48 h at indicated multiplicity of infection, respectively. Cells were treated with control shRNA (sh-CTL) or PNPT1 shRNA (sh-PNPT1) prior to viral infection. Scale bar 20 μ m. Data from three independent experiments are presented as mean \pm standard deviation. **** P <0.0001.

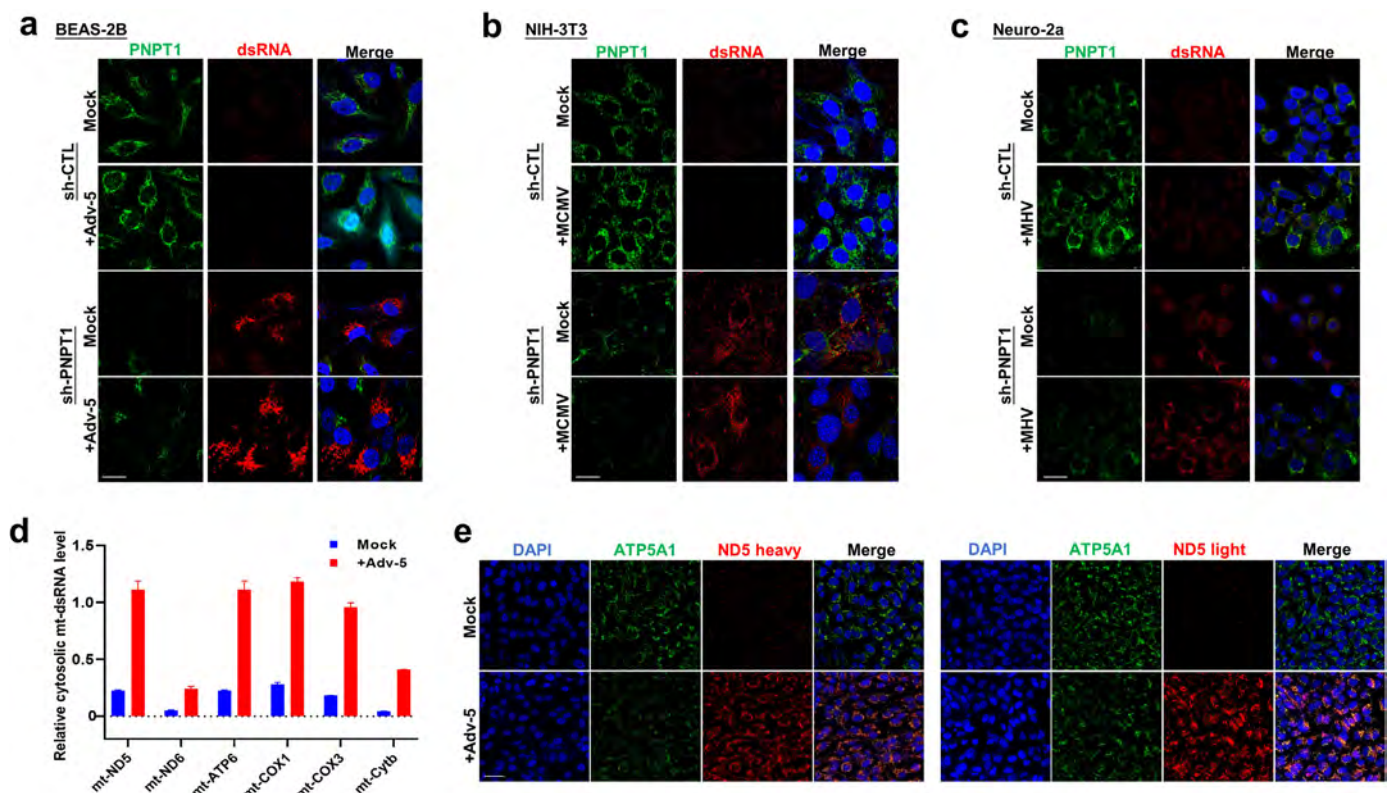


Fig. 2. A reduction in polyribonucleotide nucleotidyltransferase 1 (PNPT1) promotes relocation of mitochondria double-stranded RNAs (mt-dsRNAs) from mitochondria to cytoplasm. (a–c) Immunostaining of mt-dsRNAs (J2) in BEAS-2B cells infected or not infected with adenovirus (Adv-5) at 24 h (a), NIH-3T3 cells infected or not infected with murine cytomegalovirus (MCMV) at 48 h (b), and Neuro-2a cells infected or not infected with murine hepatitis virus (MHV-A59) at 12 h (c). Scale bar 20 μ m. (d) Quantitative reverse transcription polymerase chain reaction analysis of cytosolic mt-dsRNAs in BEAS-2B cells infected or not infected with Adv-5 at 24 h. (e) In-situ staining of cytosolic mt-ND5 heavy (left) and light strands (right) in BEAS-2B cells infected or not infected with Adv-5 at 24 h. ATP5A1 served as a mitochondria marker. Scale bar 50 μ m. Data from three independent experiments are presented as mean \pm standard deviation.

and MHV-A59 viral genes significantly at the specified time points post-infection, indicating that a high level of host cell PNPT1 is required for viral replication after the virus enters the host cells (Fig. 1g).

2.2. PNPT1 induction by viral infection prevents leakage of mt-dsRNAs to cytoplasm to initiate host cell ISR

The cellular level and distribution of dsRNAs during viral replication were examined in order to explore the mechanism underlying the role of PNPT1 in facilitating viral replication in host cells. As expected, PNPT1 levels in BEAS-2B, NIH-3T3 and Neuro-2a cells were increased following infection with Adv-5 (Fig. 2a), MCMV (Fig. 2b) or MHV-A59 (Fig. 2c), respectively. In cells treated with sh-CTL, no significant dsRNAs were detected in cytoplasm by J2 antibody [22] staining after 12 h with or without viral infection. In contrast, when the host cell PNPT1 was depleted by sh-PNPT1, abundant dsRNAs (red) were detected in the cytoplasm, even in the absence of viral infection. With viral infection, the cytosolic level of dsRNAs labelled with J2 antibody was increased markedly in PNPT1-knockdown cells. In addition, in control Neuro-2a cells infected with MHV-A59, viral dsRNA was detected in the cytoplasm by J2 antibody after 24 h of infection, suggesting the leakage of viral dsRNA into the host cell cytoplasm at a late stage of infection (Fig. S2, see online supplementary material).

A previous study showed that antiviral signalling could be initiated when mt-dsRNAs leaked into cytoplasm [15]. In order to explore the source of cytosolic dsRNAs during viral replication, dsRNAs from the mitochondria-free cytosolic fraction of BEAS-2B cells were purified using J2 antibody. In this experiment, the

mitochondria-free cytosolic fraction was isolated from BEAS-2B cells with or without viral infection, and a panel of mt-dsRNAs, including mitochondrially encoded cytochrome b (mt-Cytb), NADH dehydrogenase 5 (mt-ND5) and cytochrome c oxidase subunit 1 (mt-COX1), were quantified by quantitative reverse transcription polymerase chain reaction (qRT-PCR) with specific probes against these mt-dsRNAs. As shown in Fig. 2d, there was almost no cytosolic mt-dsRNA in non-infected cells, whereas significantly higher mRNA levels of mt-ND5/6, mt-ATP6, mt-COX1/3 and mt-Cytb were detected in cells infected with Adv-5. The in-situ fluorescence assay using specific probes against heavy and light strands of mitochondrial RNAs further confirmed a strong increase in the cytosolic mt-dsRNA level in infected cells (Fig. 2e). The results clearly show that PNPT1 is critical for controlling the leakage of mt-dsRNAs from mitochondria to cytoplasm during viral replication.

Given that cytosolic mt-dsRNAs can inhibit protein translation by binding and activating PKR [23], or by initiating an antiviral inflammatory response via recognition by RIG-I and MDA5 helicases [24], the protein synthesis capacity was examined in BEAS-2B cells with or without Adv-5 infection or PNPT1 knockdown. At 24 h post-infection with Adv-5 at different multiplicities of infection (MOI), PNPT1 knockdown in BEAS-2B cells markedly decreased the whole protein translation level (Fig. 3a). This result suggests that the role of cytosolic mt-dsRNAs in Adv-5-infected BEAS-2B cells is largely through generating the ISR to block general protein synthesis. As phosphorylation of PKR and subsequent eIF2 α are two critical components in the ISR that terminate protein translation [16], the levels of cellular PKR, eIF2 α and their phosphorylated forms (p-PKR and p-eIF2 α) with or without viral infection or PNPT1 knockdown were detected by Western blot analy-

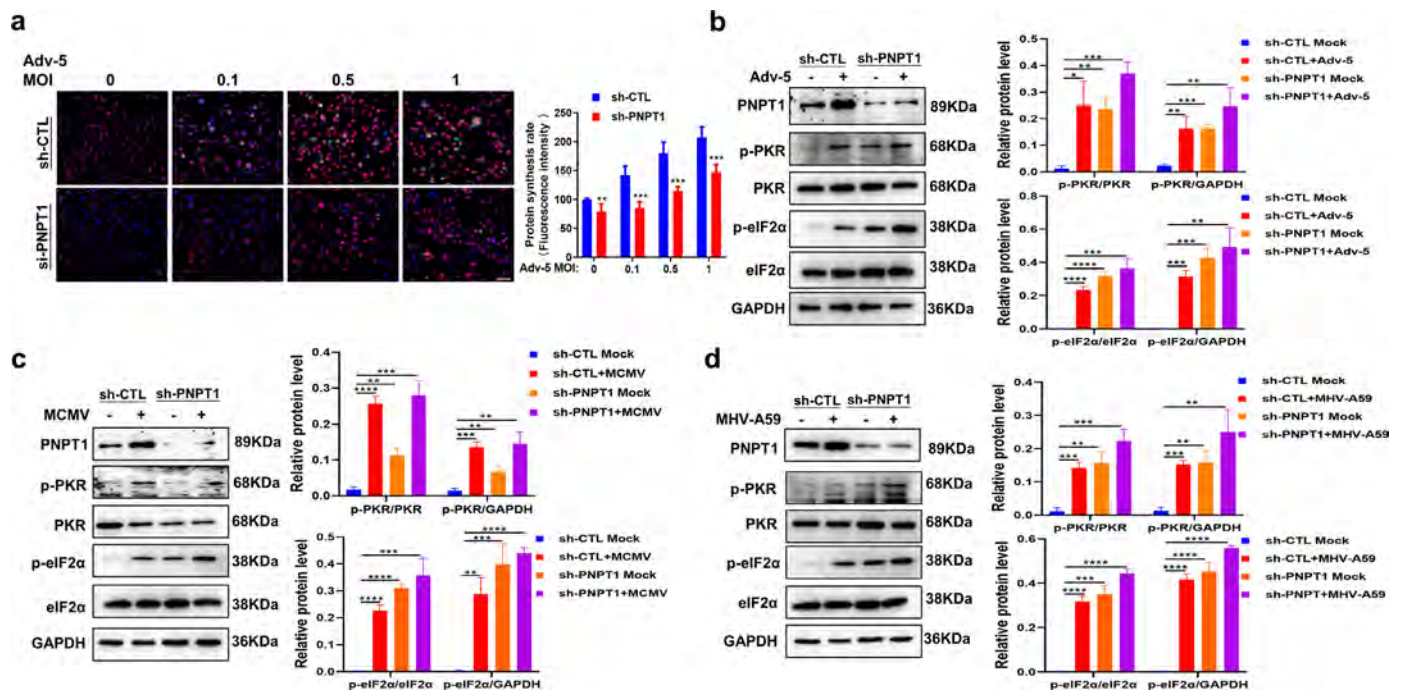


Fig. 3. Cytosolic mitochondria double-stranded RNAs activate RNA-activated protein kinase (PKR) and, subsequently, eukaryotic initiation factor 2 α (eIF2 α) to terminate general protein production. (a) Left: Fluorescence microscopy images of BEAS-2B cells infected with adenovirus (Adv-5) for 1 h, then washed with phosphate buffered saline; nascent protein synthesis at 24 h post-infection was detected by OPP-647 (red) and DAPI (blue) staining. Right: Quantification of OPP-647 staining. Scale bar, 75 μ m. (b) Western blot analysis of PNPT1, phosphorylated PKR (p-PKR), PKR, phosphorylated eIF2 α and eIF2 α levels in BEAS-2B cells infected or not infected with Adv-5 after 24 h infection. (c) Western blot analysis of PNPT1, p-PKR, PKR, p-eIF2 α and eIF2 α levels in NIH/3T3 cells infected or not infected with murine cytomegalovirus (MCMV) after 48 h infection. (d) Western blot analysis of PNPT1, p-PKR, PKR, p-eIF2 α and eIF2 α levels in Neuro-2a cells infected or not infected with murine hepatitis virus (MHV-A59) after 12 h infection. In (a–d), cells were treated with control shRNA (sh-CTL) or PNPT1 shRNA (sh-PNPT1) prior to viral infection.

sis. As shown in Fig. 3b–d, levels of p-PKR and p-eIF2 α in BEAS-2B (Fig. 3b), NIH-3T3 (Fig. 3c) and Neuro-2a cells (Fig. 3d) treated with sh-PNPT1 were markedly increased following infection with the respective viruses. The results suggest that the depletion of PNPT1 initiates the PKR-eIF2 α axis-mediated ISR in various virus-infected cells.

2.3. Identification of LanC as a potent PNPT1 inhibitor

Given that viral infection induces host cell PNPT1, which in turn facilitates pan-viral replication by suppressing the ISR mediated by the mt-dsRNA-PKR-eIF2 α signal axis, a search was undertaken for a PNPT1 inhibitor to block the replication of various viruses in the infected cells. First, PNPT1 recognition element analysis was performed, and 17,728 FDA-approved drugs and bioactive compounds were screened. As PNPT1 functions as a trimer in cleaving single-strand RNA [25], nine molecules – zofenopril calcium, fulvestrant, atazanavir sulfate, echinacoside, forsythoside B, salvianolic acid B, diquafosol tetrasodium, UNC3866 and LanC – were considered as potential PNPT1 inhibitors for blocking interaction of the PNPT1 trimer with single-strand RNA (Fig. 4a). To validate these compounds as potential PNPT1 inhibitors, cytoplasmic mt-dsRNA distribution was tested with J2 antibody after treating cells with individual compounds at 0.1–10 μ M for 24 h (Fig. 4b). Compared with BEAS-2B cells without treatment, in which no apparent staining of mt-dsRNAs was observed, there was strong J2 antibody labelling of mt-dsRNAs in the cytoplasm of BEAS-2B cells treated with LanC, as well as those treated with salvianolic acid B and atazanavir sulfate although to a much lesser degree (Fig. 4c). Next, the inhibitory effect of these bioactive compounds, at various concentrations, on Adv-5 replication in BEAS-2B cells was tested (Fig. 4d). The half-maximal inhibitory concentration (IC₅₀) values of individual compounds used in the experiments were determined (Fig. S3, see on-

line supplementary material). Among these selected bioactive compounds, LanC had the strongest inhibitory effect on the replication of Adv-5 (MOI of 0.5) in BEAS-2B cells at 24 h post-infection (Fig. 4e). Consistent with the inhibitory efficacy on virus replication, the level of mt-dsRNAs in the cytoplasm of BEAS-2B cells treated with LanC was significant, suggesting that LanC suppresses virus replication by inhibiting PNPT1. Furthermore, active PNPT1-trimer (Fig. 4f, insert) was purified, and micro-scale thermophoresis (MST) was performed to measure the binding capacity of LanC-PNPT1 (Fig. 4f). In line with the observation of cellular mt-dsRNA staining by J2 antibody, LanC displayed high affinity with the purified PNPT1 trimer, with K_d of $0.419 \pm 0.133 \mu$ M. Additionally, the precise binding assay involving recombinant PNPT1 and Cy5-labelled single-strand RNA (Cy5-ssRNA), as measured by MST, validated the specific inhibitory effect of LanC on the PNPT1-ssRNA interaction (Fig. S4, see online supplementary material). Complementing this, molecular docking analysis provided insightful details into the potential interaction between PNPT1 and LanC, as depicted in Fig. S5 (see online supplementary material).

2.4. LanC blocks pan-viral replication via activating mt-dsRNA-PKR-eIF2 α axis

The effect of LanC on blockade of the replication of the three viruses in their respective host cells was examined. In this experiment, BEAS-2B, NIH3T3 and Neuro-2a cells were infected with Adv-5, MCMV and MHV-A59 at MOI of 0.01, 0.5, 1.0, respectively. Cells were then treated with or without LanC at the indicated concentration for 24 h. The effects of suppression on viral replication were analysed quantitatively using qRT-PCR. As shown in Fig. 5a–c, the replication of Adv-5 (Fig. 5a), MCMV (Fig. 5b) and MHV-A59 (Fig. 5c) was inhibited in a dose-dependent manner by LanC. No significant cell toxicity was observed for LanC at 50% effective con-

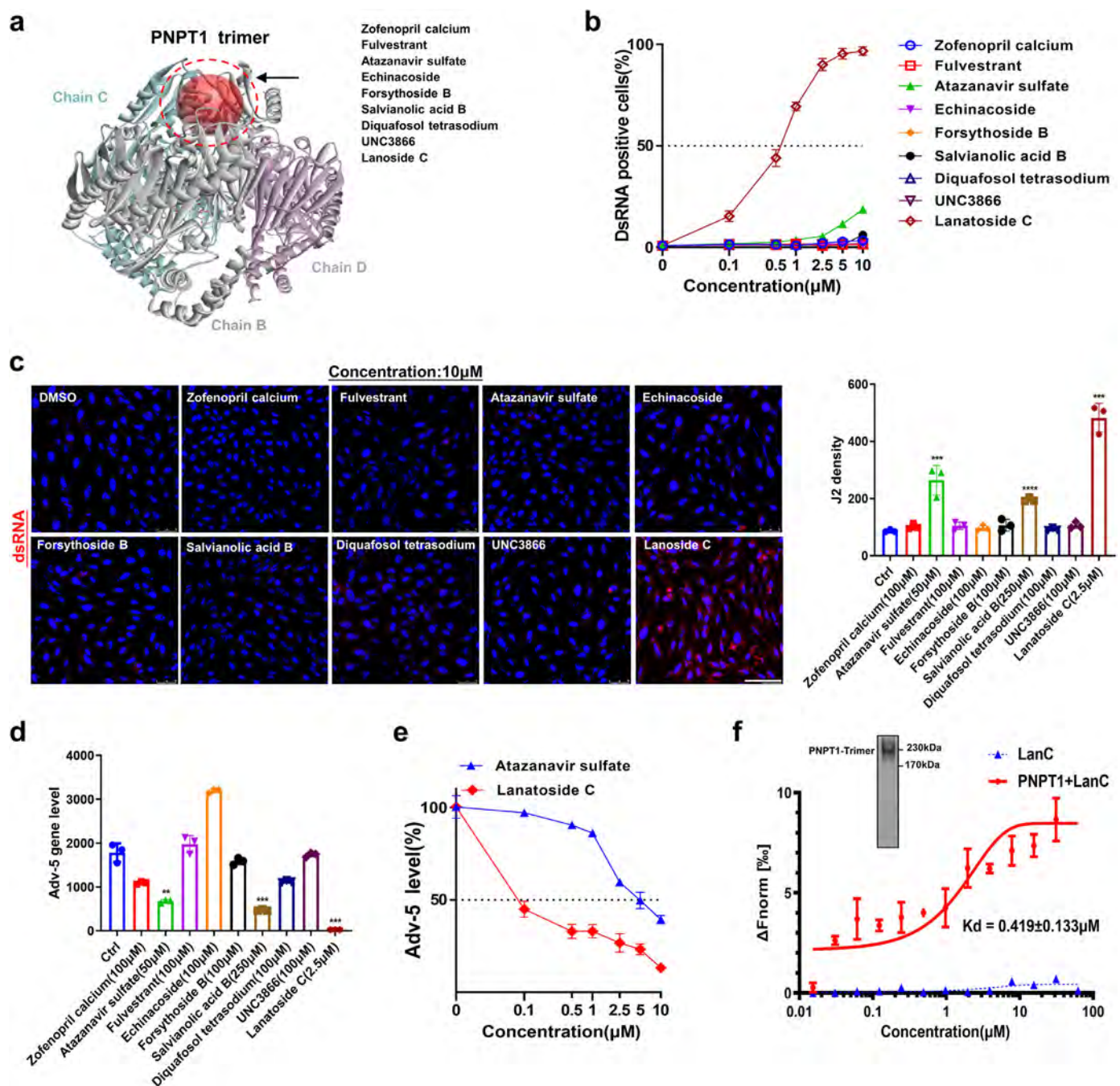


Fig. 4. Identification of lanatoside C (LanC) as a potent inhibitor of polyribonucleotide nucleotidyltransferase 1 (PNPT1) using bioactive compounds approved by the US Food and Drug Administration. (a) Prediction of PNPT1 inhibition based on functional PNPT1 structural analysis. (b) BEAS-2B cells were infected with adenovirus (Adv-5) at multiplicity of infection (MOI) of 0.5 and treated with various compounds at indicated concentrations for 24 h. The effects of each compound on induction of cellular mitochondria double-stranded RNAs (mt-dsRNAs) labelled with J2 antibody were analysed by immunofluorescence staining. (c) Left: Representative images of cellular mt-dsRNA staining by J2 antibody as a readout for PNPT1 inhibition (red, mt-dsRNA; blue, nuclei). Scale bar 50 μm. Right: Quantification of cellular mt-dsRNAs labelled with J2 antibody was analysed by immunofluorescence staining. (d) BEAS-2B cells were infected with Adv-5 at MOI of 0.5 and treated with different compounds at indicated concentrations for 24 h. The inhibition of viral replication was analysed using quantitative reverse transcription polymerase chain reaction. (e) Dose-dependent inhibition of LanC and atazanavir sulfate on Adv-5 replication (MOI of 0.5) in BEAS-2B cells. (f) Micro-scale thermophoresis analysis of binding affinity of LanC with functional PNPT1 trimer. Data from three independent experiments are presented as mean ± standard deviation. ** $P < 0.01$, *** $P < 0.001$.

centration (EC_{50}) values (Fig. S6, see online supplementary material).

To test whether the inhibition of viral propagation by LanC is by initiating the host cell ISR, BEAS-2B cells were treated with 0.5 μM LanC or DMSO vehicle for 24 h, and mt-dsRNA staining was examined by J2 antibody. BEAS-2B cells were infected, or not infected, with Adv-5 at MOI of 0.5 prior to LanC treatment. As shown in Fig. 6a, LanC treatment strongly increased the cellular distribution

of mt-dsRNAs (red), especially in the Adv-5-infected BEAS-2B cells. Consistently, the mitochondria-free cytosolic fraction from LanC-treated BEAS-2B cells contained significantly more mt-dsRNAs than the CTL cells (Fig. 6b,c). Western blot analysis showed that LanC treatment enhanced the levels of p-PKR and p-eIF2α in a dose-dependent manner in BEAS-2B cells infected with Adv-5 (Fig. 6d). In agreement with the notion that phosphorylation of eIF2α leads to termination of general protein translation [26], a total protein

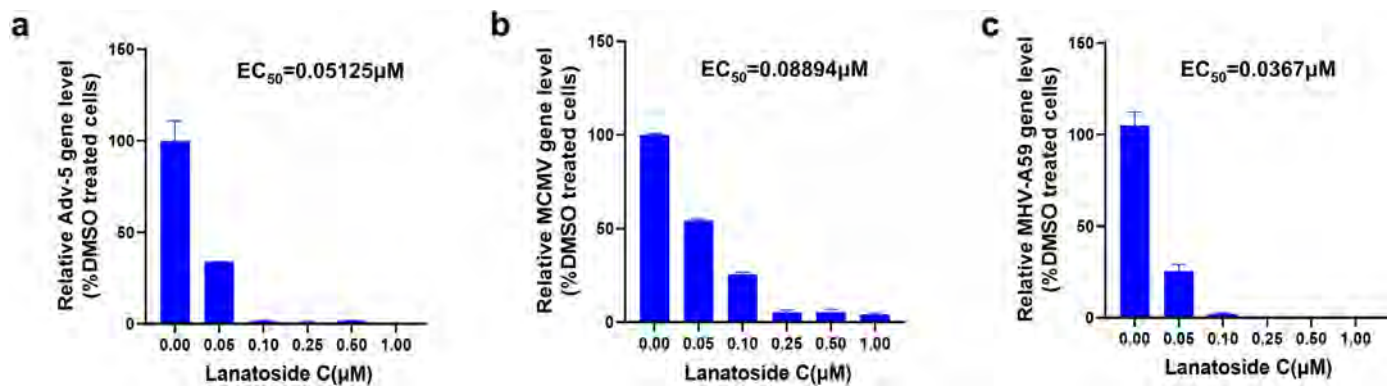


Fig. 5. Inhibition of polyribonucleotide nucleotidyltransferase 1 activity by lanatoside C (LanC) in host cells suppresses replication of adenovirus (Adv-5), murine cytomegalovirus (MCMV) and murine hepatitis virus (MHV-A59). (a) BEAS-2B cells were infected with Adv-5 at multiplicity of infection (MOI) of 0.5 and treated with LanC at indicated concentrations for 24 h. The effects of suppression of viral replication were analysed quantitatively using quantitative reverse transcription polymerase chain reaction (qRT-PCR). (b) NIH-3T3 cells were infected with MCMV at MOI of 1 and treated with LanC at indicated concentrations for 48 h. The effects of suppression of viral replication were analysed quantitatively using qRT-PCR. (c) Neuro-2a cells were infected with murine hepatitis virus (MHV-A59) at MOI of 0.01 and treated with LanC at indicated concentrations for 12 h. The effects of suppression of viral replication were analysed quantitatively using qRT-PCR. Data from three independent experiments are presented as mean \pm standard deviation.

synthesis assay showed that LanC treatment reduced total protein synthesis in a dose-dependent manner, especially in Adv-5-infected BEAS-2B cells (Fig. 6e).

As LanC is capable of inhibiting the replication of various viruses by blocking general protein synthesis in the infected cells, this study tested whether LanC treatment can prevent production of SARS-CoV-2 S-protein in infected cells. In this experiment, BEAS-2B cells were infected with SARS-CoV-2 pseudo-virions at MOI of 0.01, and treated with LanC at the indicated concentration for 24 h. As shown, LanC treatment blocked S-protein synthesis at both mRNA (Fig. 7a) and protein (Fig. 7b) level. In a similar manner, Western blot analysis indicated that LanC treatment decreased the S-protein level, but increased the p-PKR and p-eIF2 α levels in a dose-dependent manner in BEAS-2B cells at 24 h post-infection (Fig. 7c). Taken together, these results suggest that, by activating the mt-dsRNA-PKR-eIF2 α signal axis in the virus-infected cells, the PNPT1 inhibitor LanC effectively blocks pan-viral replication as well as SARS-CoV-2 S-protein production.

3. Discussion

Using multiple viral infection systems, this study demonstrated that upregulation of host cell PNPT1 expression and activity serves as a common strategy for various viruses to resist the cellular ISR induced by the mt-dsRNA-PKR-eIF2 α signal axis, whereas pan-viral propagation in infected cells can be achieved by inhibiting host cell PNPT1.

In the development of antiviral strategies against various viral infections, particularly SARS-CoV-2, the majority of research has focused directly on viruses rather than host cells [27–29]. The viral factors that govern how viruses enter host cells, and how viruses replicate in host cells have been explored extensively [30,31]. However, significantly less attention has been paid to infected cells, which also play a critical role in viral infection. Indeed, viruses have developed different mechanisms to infect their respective host cells; however, after entering the host cells, all viruses must hijack the host cell protein synthesis machinery to produce viral components in order to replicate. An increase in viral protein production in host cells places major stress on the mitochondria of host cells, resulting in an enhanced ISR which could terminate general protein synthesis. In line with the notion that the ISR serves as a general antiviral host defence, this study found that the leakage of a large amount of mt-dsRNAs into cytoplasm, induced by viral infection, could initiate a strong ISR which blocks viral repli-

cation. In cytoplasm, mt-dsRNAs rapidly bind to and activate PKR, which, in turn, phosphorylates eIF2 α , leading to the termination of general protein translation. As shown in Fig. 2d, the whole protein synthesis rate in BEAS-2B cells infected with Adv-5 at various MOI was reduced significantly by depleting PNPT1. This result argues that, in cases of viral infection, instead of being recognized by RIG-I and MDA5 and activating pro-inflammatory signalling, cytosolic mt-dsRNAs activate PKR and initiate the ISR to terminate the protein synthesis. These results also show that viruses can markedly upregulate PNPT1 in host cells to prevent the leakage of mt-dsRNAs into cytoplasm. As a major mammalian cell 3'-to-5' exoribonuclease, PNPT1 is mainly associated with mitochondria and, through collaboration with SUV3, PNPT1 maintains the homeostasis of mitochondria RNAs in the host cells [25]. By promoting PNPT1 expression to cleave mt-dsRNAs, viruses can successfully minimize the ISR induced by the mt-dsRNA-PKR-eIF2 α signal axis.

How mt-dsRNAs are released from mitochondria to cytoplasm following viral infection remains unknown. A previous study by McArthur et al. showed that Bcl-associated X protein (BAX) and Bcl-2 homologous antagonist/killer (BAK) complex played an important role in mitochondrial apoptosis by enhancing mitochondrial permeability and the efflux of pro-apoptotic factors, such as cytochrome c and mitochondrial DNAs [32]. Their morphological study revealed that macropores formed by the BAX/BAK complex may mediate the leakage of mitochondrial DNAs to the cytoplasm during cell apoptosis. In cells lacking PNPT1 enzymatic activity, mt-dsRNAs are likely released from mitochondria to cytoplasm in a similar mechanism of mt-DNA leakage. This hypothesis is supported by the observation that depletion of either BAX or BAK markedly blocks the upregulation of IFN β 1 mRNA upon PNPase knockdown [33], suggesting that mt-dsRNA leakage may depend upon BAX/BAK mitochondrial pores. The role of BAX/BAK complex in leakage of mitochondrial nucleic acids, including mt-dsRNAs, to the cytoplasm was confirmed recently by Tigano et al. [34]. Interestingly, an early PNPase study in melanoma cells also found that PNPase could affect the level of BCL-xL, an agonist of BAX that prevents pore formation on outer mitochondrial membranes [35], arguing that PNPT1 may regulate mt-dsRNA efflux by not only cleaving mt-dsRNAs as an exoribonuclease, but also by influencing the formation of BAX/BAK pores.

Given the important role of PNPT1 in controlling the ISR and maintaining viral replication, the authors attempted to establish a strategy to prevent the replication of various viruses by the inhi-

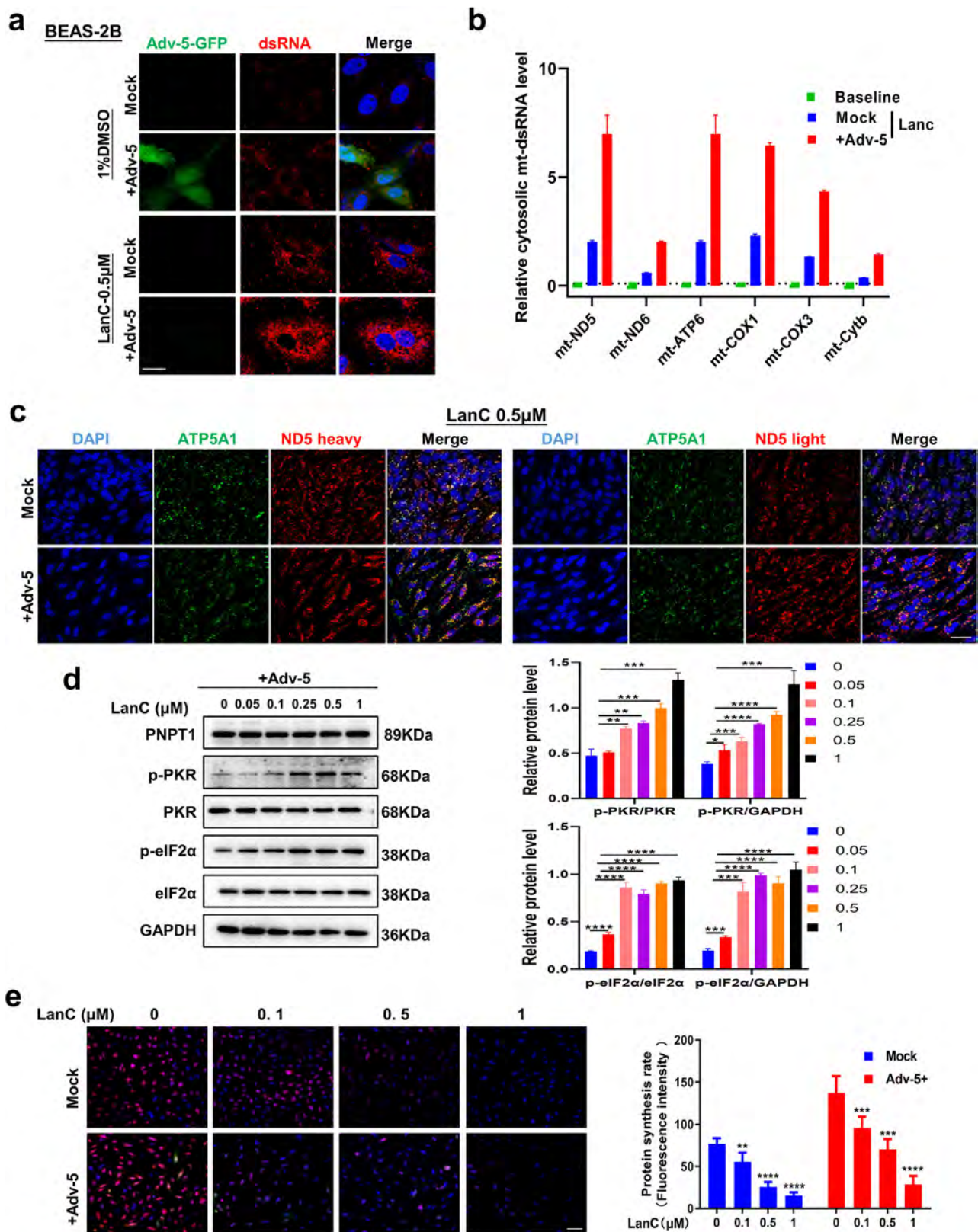


Fig. 6. Lanatoside C (LanC), an inhibitor of polyribonucleotide nucleotidyltransferase 1 (PNPT1), suppresses virus replication by activating RNA-activated protein kinase (PKR) and, subsequently, eukaryotic initiation factor 2 α (eIF2 α). (a) Immunostaining of double-stranded RNA (red) in BEAS-2B cells treated with LanC at indicated concentration for 24 h. Scale bar 20 μ m. (b) Quantitative reverse transcription polymerase chain reaction analysis of cytosolic mitochondria double-stranded RNAs (mt-dsRNAs) in BEAS-2B cells infected and not infected with adenovirus (Adv-5). (c) In-situ staining of cytosolic mt-ND5 heavy (left) and light strands (right) in BEAS-2B cells infected and not infected with Adv-5. ATP5A1 served as a mitochondria marker. Scale bar 50 μ m. (d) Western blot analysis of PNPT1, p-PKR, PKR, p-eIF2 α and eIF2 α expression in BEAS-2B cells treated with LanC at indicated concentrations for 24 h. (e) Left: Fluorescence microscopy images of BEAS-2B cells infected with Adv-5 virus for 1 h, washed with phosphate buffered saline, then treated with LanC at indicated concentrations for another 24 h; nascent protein synthesis was detected by staining with OPP-647 (red), and genomic DNA was stained using DAPI (blue). Right: Quantification of OPP-647 staining. Scale bar 50 μ m. Data from three independent experiments are presented as mean \pm standard deviation. * P <0.05, ** P <0.01, *** P <0.001, **** P <0.0001.

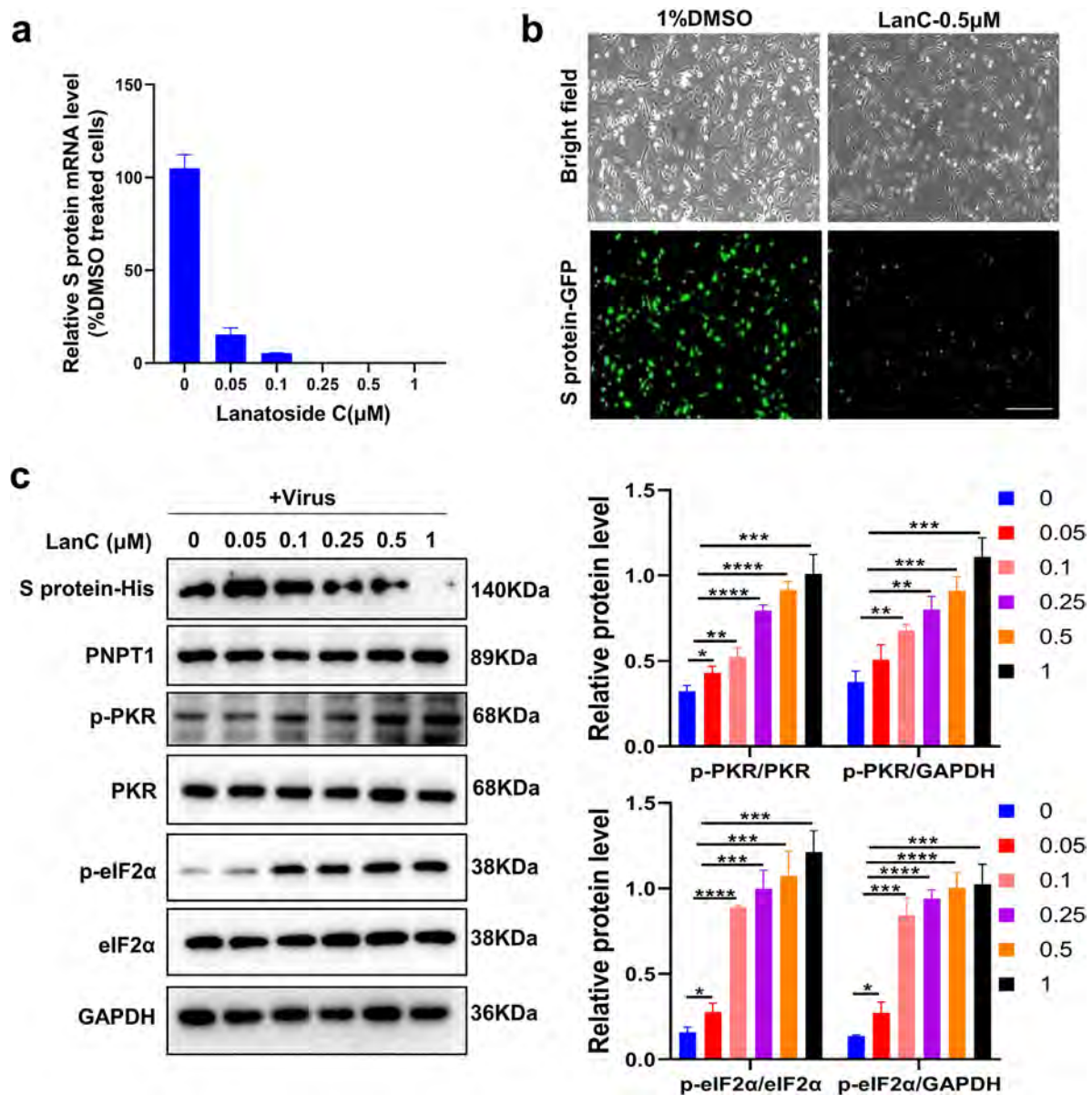


Fig. 7. Lanatoside C (LanC) suppresses production of severe acute respiratory syndrome coronavirus-2 (SARS-CoV-2) spike (S) protein in BEAS-2B cells. BEAS-2B cells were infected with SARS-CoV-2 pseudo-virions at multiplicity of infection of 0.01, and treated with LanC at indicated concentrations for 24 h. (a) The effects of suppression of viral replication were analysed quantitatively using quantitative reverse transcription polymerase chain reaction. (b) The effects of suppression of viral replication were detected with green fluorescent protein (GFP). (c) Western blot analysis of S-protein, polyribonucleotide nucleotidyltransferase 1 (PNPT1), phosphorylated RNA-activated protein kinase (p-PKR), PKR, phosphorylated eukaryotic initiation factor 2α (p-eIF2α) and eIF2α expression after LanC treatment. Data from three independent experiments are presented as mean ± standard deviation. * $P < 0.05$, *** $P < 0.001$, **** $P < 0.0001$.

bition of host cell PNPT1 activity. Through PNPT1 structural analysis, mt-dsRNA tracing by J2 antibody and functional assays, LanC was identified as a potent PNPT1 inhibitor. Although the underlying mechanism remains completely unknown, LanC has been used previously to treat patients with various viral infections, including dengue virus, flavivirus Kunjin, alphavirus Chikungunya, sindbis virus and enterovirus 71, and has an inhibitory effect on virus infection [36,37]. In line with the present authors' suggestion that LanC binds to PNPT1, MST shows high affinity of LanC with purified recombinant PNPT1 (Fig. 4d), and LanC inhibits the binding of recombinant PNPT1 with fluorescently labelled ssRNA in a dose-dependent manner (Fig. S4, see online supplementary material). LanC is effective for viral inhibition in infected cells at doses well below the Kd value derived from the binding assays using recombinant PNPT1. The main reason for this may be the poor ability of purified recombinant PNPT1 to form a functional trimer. LanC

treatment markedly enhances the distribution of mt-dsRNAs in the cytoplasm of host cells (Fig. 6a). Western blot analysis further confirmed the increase in phosphorylated PKR and eIF2α induced by LanC (Fig. 6d). As depicted in Fig. 8, viral infection upregulates PNPT1, which controls mt-dsRNAs and their leakage from mitochondria to cytoplasm during viral replication. LanC suppresses viral replication by increasing mt-dsRNAs in cytoplasm, where mt-dsRNAs activate the PKR-eIF2α signal axis and inhibit general protein synthesis and viral replication. As shown, LanC treatment promoted cytoplasmic mt-dsRNA distribution significantly during viral infection (Fig. 6a–c), and blocked the replication of Adv-5, MCMV and MHV (Fig. 5), as well as the production of SARS-CoV-2 S-protein (Fig. 7a,b), in a dose-dependent manner. In summary, as PNPT1 induction is deployed by various viruses as a critical survival strategy to suppress the ISR induced by the mt-dsRNA-PKR-eIF2α axis during viral infection, the identification of LanC as a

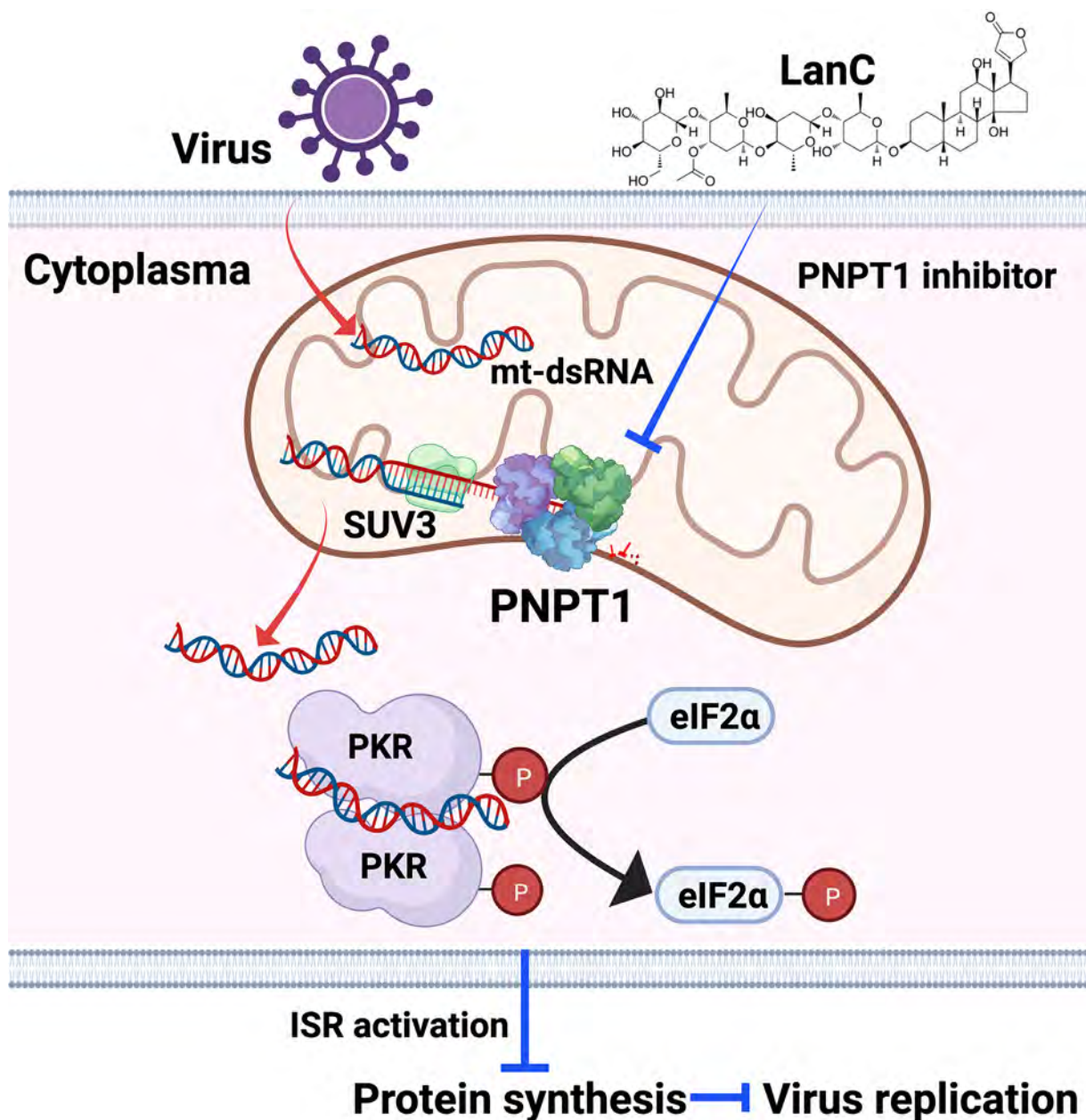


Fig. 8. Schematic working model of lanatoside C (LanC), an inhibitor of polyribonucleotide nucleotidyltransferase 1 (PNPT1), blocking pan-viral replication in host cells. PKR, RNA-activated protein kinase; eIF2 α , eukaryotic initiation factor 2 α .

PNPT1 inhibitor may provide an effective treatment to block pan-viral replication.

4. Materials and methods

4.1. Cells and viruses

BEAS-2B, HEK293T, NIH-3T3 and Neuro-2a cell lines were purchased from the Shanghai Institute of Cell Biology, Chinese Academy of Sciences, Shanghai, China. These cell lines were cultured in DMEM medium (Thermo Fisher, Waltham, MA, USA) supplemented with 10% fetal bovine serum (Thermo Fisher), 100 U/mL penicillin and streptomycin (Thermo Fisher), and maintained at 37°C in a humidified atmosphere at 5% CO₂. MCMV was a laboratory-adapted strain provided by Professor Fenyong Liu from the University of California at Berkeley, CA, USA, and propagated in

NIH-3T3 cells. MHV-A59 was provided by Professor Rong Ye of Fudan University, Shanghai, China, and propagated in Neuro-2a cells. The COVID-19 S pseudovirions were purchased from Tsingke, Beijing, China.

4.2. Western blot analysis

Whole-cell extracts of indicated cultured cells were lysed using RIPA buffer (Beyotime, Haimen, China) containing 1mM PMSF (Beyotime), and 1% protease and phosphatase inhibitor cocktail (Thermo Fisher) on ice for 30 min. The samples were centrifuged at 13,000 rpm for 10 min at 4°C to collect the supernatant. The protein concentration of supernatant was quantified using a Pierce BCA protein assay kit (Thermo Fisher Scientific) in accordance with the manufacturer's instructions. Equal quantities of proteins were mixed with SDS loading buffer (Beyotime) and heated for 5 min at

95°C. Prepared samples were separated on 10% SDS-PAGE and then transferred to PVDF membranes (Millipore, Schwalbach, Germany). The membranes were blocked in 5% non-fat milk diluted in Tris-buffered saline with 0.1% Tween 20 detergent for 1 h at room temperature. Primary antibodies against PKR (18244-1-AP; Proteintech, Rosemont, IL, USA), p-PKR (ab32036; Abcam, Cambridge, UK), eIF2 (#5324; Cell Signaling Technology, Danvers, MA, USA), p-eIF2α (#3398; Cell Signaling Technology), PNPT1 (14487-1-AP; Proteintech), ATP5A1 (14676-1-AP; Proteintech), His-tag (66005-1-Ig; Proteintech) or GAPDH (sc-25778, Santa Cruz Biotechnology) were used. The horseradish peroxidase (HRP)-conjugated anti-mouse immunoglobulin (IgG) antibody (115-005-003; Jackson ImmunoResearch, West Grove, PA, USA) and the HRP-conjugated anti-rabbit IgG antibody (111-035-144; Jackson ImmunoResearch) were used as secondary antibodies. Immunoreactivity was visualized with an ECL-Plus kit (Thermo Fisher Scientific) using the ChemiDoc MP system (Bio-Rad, Hercules, CA, USA).

4.3. Immunofluorescence staining

Immunofluorescence labelling was performed to identify the intracellular level and distribution of mt-dsRNAs and PNPT1. After different periods post-siRNA transfection or viral infection, cells were briefly fixed with 4% paraformaldehyde and subsequently permeabilized with 0.25% (w/v) Triton X-100 for 15 min. Cells were blocked in 3% (w/v) bovine serum antigen diluted in phosphate buffered saline (PBS) solution for 30 min, and then incubated overnight with the monoclonal anti-dsRNA J2 antibody (10010200; Scicons, Susteren, The Netherlands) and PNPT1 polyclonal antibody (14487-1-AP; Proteintech), followed by incubation with fluorophore-tagged secondary antibodies (Thermo Fisher). All samples were stained with DAPI (Beyotime) for nuclear labelling. A Leica confocal microscope was used for cell imaging. For screening PNPT1 inhibitors, cell images were acquired using high content screening (Operetta; Perkin Elmer, Shelton, CT, USA) and analysed by Columbus analysis software.

4.4. Plasmid and siRNA transfection

The shRNA plasmids designed to specifically repress the expression of PNPT1 were purchased from GeneCopoeia (Guangzhou, China). An empty plasmid served as a negative control. The sequences of siRNA are provided in Table S1 (see online supplementary material). Gene-specific siRNAs and a scrambled siRNA (control) were purchased from RiboBio (Guangzhou, China). The siRNAs and plasmids were transfected into the indicated cells using lipofectamine 3000 (Invitrogen, Waltham, MA, USA) in accordance with the manufacturer's instructions. Total DNA, RNA and protein were isolated at the indicated times after transfection, and assessed by qRT-PCR or Western blotting.

4.5. DNA/RNA extraction and qRT-PCR assay

Genomic DNA was extracted from cells using a commercially genomic DNA extraction kit in accordance with the manufacturer's instructions (DP304; Tiangen, Beijing, China). Total RNA was isolated from cells using TRIzol reagent (Thermo Fisher) in accordance with the manufacturer's protocol, and 1 µg RNA was reverse transcribed into cDNA by HiScript III RT SuperMix for qPCR (+gDNA wiper) (Vazyme, Nanjing, China) in accordance with the manufacturer's instructions. Gene expression was analysed using ChamQ Universal SYBR qPCR Master Mix (Vazyme) with the LightCycler 96 qPCR system (Roche Diagnostics, Mannheim, Germany) in accordance with the manufacturer's specifications. The reactions were started with incubation at 95°C for 5 min, followed by 40 cycles of

95°C for 15 s and 60°C for 1 min. The qRT-PCR primers are listed in Table S2 (see online supplementary material).

4.6. Detection of mt-dsRNAs in cytosolic fraction

The treated BEAS-2B cells (1×10^8) were resuspended in 1 mL lysis buffer (150 mM NaCl, 50 mM HEPES, 25 µg/mL digitonin, pH 7.4) on ice for 10 min, then centrifuged at 1000 g three times for 3 min each time to obtain the supernatants, and then spun at 17,000 g for 10 min, yielding cytosolic preparations free of mitochondrial contamination [38]. Western blot experiments were performed to confirm the enrichment cytoplasm fraction in isolated products (Fig. S7, see online supplementary material). To detect the amount of mt-dsRNAs in the cytosolic fraction, immunoprecipitation assays using J2 antibody were performed using the Pierce™ Classic IP Kit. dsRNA was isolated using TRIzol reagent and subjected to strand-specific RT-qPCR analysis. The RT primers and qRT-PCR primers were designed to target the specific genes, and are listed in Table S2 (see online supplementary material).

4.7. RNA fluorescent in-situ hybridization

To visualize heavy and light strands of mt-ND5 RNA, RNA fluorescent in-situ hybridization was performed using a Fluorescent In Situ Hybridization Kit (RiboBio) in accordance with the manufacturer's protocol. Briefly, cells were cultured in 24-well plates lined with microscope cover glass, treated with indicated conditions, fixed with 4% paraformaldehyde for 10 min, and subsequently permeabilized with pre-cold 0.5% (w/v) Triton X-100 in PBS buffer for 10 min. After washing with cold PBS buffer three times, the cells were blocked with pre-hybridization buffer for 30 min at 37°C, and incubated with probe hybridization buffer overnight at 37°C protected from light. The following day, cells were washed with different concentrations of SSC buffer and then stained with DAPI (Beyotime) for nuclear labeling. A Leica confocal microscope was used for cell imaging.

4.8. Total protein synthesis assays

The rate of protein synthesis was examined by monitored the synthesis of O-propargyl-puromycin, an analogue of puromycin that contains a terminal alkyne group using a Click-iT Plus OPP Alexa Fluor 647 Kit (C10458; Thermo Fisher). Briefly, 20 µM O-propargyl-puromycin (OPP) was added to the cells and incubated for 30 min. Cells were washed in ice-cold PBS and then fixed and permeabilized. Next, Alexa-Fluor-647 was conjugated to OPP following the manufacturer's instructions, and cells were stained with DAPI.

4.9. Virtual screening

The crystal structure of human PNPT1 (PDB ID: 3U1K) was retrieved from the Research Collaboratory for Structural Bioinformatics Protein Data Bank (RCSB PDB) website. The Cofactor server [39] was employed to explore the biochemical functions and potential binding regions for PNPT1 antagonists. A diverse library of 17,728 compounds, sourced from Selleck, encompassing the FDA-approved Drug Library (2682 compounds), Drug Repurposing Library (2826 compounds), Bioactive Compound Library-I (6911 compounds) and Bioactive Compound Library-II (5309 compounds), was screened. Initially, a grid box was positioned strategically to encompass the active site of the crystal structure. Subsequently, the calculation of binding energies was executed using PyRx AutoDock VINA. The top-ranked compounds were subjected to further analysis utilizing AutoDock [40]. Ultimately, the findings were analysed comprehensively using the Discovery Studio and PyMOL programs.

4.10. Molecular docking analysis

The Glide module of the Schrödinger software suite [41] was used to predict the binding interaction between PNPT1 and LanC. The PNPT1 model (3U1K) was obtained from RCSB PDB and prepared using Maestro. Protein preparation steps included adding missing hydrogens, removing water molecules and ions, and subsequently minimizing the protein structure using the OPLS3e force field. LanC was downloaded from the National Center for Biotechnology Information, and generated as a ligand using the Builder tool in PyMOL. For the docking parameters, Van der Waals radii were scaled to 0.8, and a partial charge cut-off was set to 0.15. The docking task was conducted using standard precision for peptides without specifying the active site residues of PNPT1. Following completion of the docking process, the resulting poses were examined thoroughly to evaluate the specificity between PNPT1 and LanC.

4.11. Cell Counting Kit-8 assay

The Cell Counting Kit-8 (CKK-8) assay was used to assess cell viability. In brief, cells were seeded into a 96-well plate overnight in order to adhere, followed by treatment with different serially diluted PNPT1 inhibitors (MedChemExpress, Monmouth Junction, NY, USA) for another 24 h. Next, each well was supplemented with 100 μ L cell culture medium containing 10% CKK-8 reagent (APExBio, Houston, TX, USA). The plate was incubated for 2 h. Finally, absorbance at 450 nm was measured using a microplate reader (Bio-Rad).

4.12. Recombinant PNPT1 protein expression and purification

The genes of human PNPT1 coding regions (residues 46–783) were cloned into pET-21a plasmid and confirmed by DNA sequencing. The pET-21a plasmid, carrying the PNPT1 encoding sequence (residues 46–783), was expressed in *Escherichia coli* BL21 cells. The bacterial culture was grown overnight at 37°C in Luria–Bertani media supplemented with 50 μ g/mL kanamycin. Once the optical density at 600 nm reached 0.8, the cells were induced by adding 0.5 mM isopropyl β -D-thiogalactoside, and further cultured at 16°C for an additional 20 h. After incubation, the bacteria containing the recombinant PNPT1 protein were harvested by centrifugation and then subjected to sonication in cold lysis buffer (50 mM Tris-HCl, pH 8.0, 500 mM NaCl, 5 mM imidazole, 1 mM TCEP and 1% complete EDTA-free protease inhibitor tablets). Subsequently, the lysate was centrifuged at 15,000 g for 45 min at 4°C. The supernatant was loaded on to a chromatography column packed with Ni Sepharose 6 Fast Flow beads (GE Life Sciences, Chicago, IL, USA) in working buffer (50 mM Tris-HCl, pH 8.0, 500 mM NaCl, 5 mM imidazole and 1 mM TCEP). PNPT1 protein was then eluted with working buffer containing 250 mM imidazole. The eluted protein was further purified using a gel filtration Superdex 200 column (GE Life Sciences) in fast protein liquid chromatography buffer (50 mM Tris-HCl, pH 8.0, 150 mM NaCl, 1 mM TCEP). The fraction containing PNPT1 trimer protein was pooled and verified by Native-PAGE.

4.13. Microscale thermophoresis analysis

For MST analysis, purified PNPT1 trimer was labelled with Monolith NT-647-NHS. The labelled protein was utilized at a concentration of 100 nM in a buffer composed of 50 mM Tris-HCl and 150 mM NaCl at pH 8.0, containing 0.05% Tween 20. The concentration of LanC varied within the range of 15 nM to 62.5 μ M. After incubating the labelled protein with the inhibitors for 20 min, the mixture was transferred into silicon-treated capillaries. Thermophoresis was measured for 30 s using a NanoTemper Monolith

NT.115 instrument (NanoTemper Technologies, Munich, Germany), with 60% LED power and 20% laser power settings. The dissociation constant was calculated using the mass action equation (Kd formula) through NanoTemper Analysis 1.5.41 software.

4.14. Inhibition of PNPT1-ssRNA binding by LanC

The 5 \hat{C} y5-labelled ssRNA (Cy5- CUAUUGCACCAGGCCAGAUGA-GAGAACCAAGGGGAAGUGACAU) (5 \hat{C} y5-ssRNA) was purchased from Tsingke. Purified PNPT1 protein (from 0.06 to 2000 nM) was incubated with equal volumes (10 μ L) of 5 \hat{C} y5-ssRNA (10 nM final concentration) in binding buffer (10mM Tris, 50 mM KCl, 1 mM DTT, 10 mM EDTA, 0.05% Tween 20, pH 8.0) for 15 min at room temperature. LanC (from 0.024 to 400 μ M) was added to the mixture of 120 nM recombinant PNPT1 and 10 nM 5 \hat{C} y5-ssRNA in 20 μ L binding buffer for 15 min at room temperature. The binding of recombinant PNPT1 with 5 \hat{C} y5-ssRNA was analysed by MST.

4.15. Statistical analysis

All Western blot images are representative of at least three independent experiments. The qRT-PCR and cytotoxicity assays were performed in triplicate, and each individual experiment was repeated several times. Data are presented as mean \pm standard deviation. Observed differences were considered significant at $P < 0.05$ using Student's *t*-test or two-way analysis of variance. All analyses were performed with GraphPad Prism v.9.0.0 (GraphPad Software, San Diego, CA, USA).

4.16. Data availability

Uncropped Western blot images and statistical source data are provided with this paper. Further supporting data are available upon request to the corresponding authors.

Acknowledgements

The authors wish to thank Prof. Rong Ye from Fudan University for the generous gift of MHV-A59. In addition, the authors wish to thank Dr. Bo Peng from Tsinghua University for kind assistance in conducting the molecular docking analysis of PNPT1 and LanC.

Author contributions: Ke Zen and Hongwei Liang designed the experiments. Shuang Qu, Chen Yang, Xinlei Sun, Hai Huang, Jiacheng Li and Yujie Zhu performed the experiments and analysed the data. Yaliang Zhang screened and analysed the potential inhibitors binding to PNPT1. Ke Zen and Shuang Qu wrote the paper.

Funding: This work was supported by grants from the [Ministry of Science and Technology of China \(2018YFA0507100\)](#), [National Natural Science Foundation of China \(82170692\)](#), [China Postdoctoral Science Foundation \(2021M703595\)](#), and Jiangsu Funding Programme for Excellent Postdoctoral Talent (2022ZB284).

Competing interests: None declared.

Supplementary materials

Supplementary material associated with this article can be found, in the online version, at [doi:10.1016/j.ijantimicag.2024.107124](https://doi.org/10.1016/j.ijantimicag.2024.107124).

References

- [1] Bomsel M, Alfsen A. Entry of viruses through the epithelial barrier: pathogenic trickery. *Nat Rev Mol Cell Biol* 2003;4:57–68.
- [2] Grove J, Marsh M. The cell biology of receptor-mediated virus entry. *J Cell Biol* 2011;195:1071–82.

- [3] Su YC, Wu JL, Hong JR. Betanodavirus up-regulates chaperone GRP78 via ER stress: roles of GRP78 in viral replication and host mitochondria-mediated cell death. *Apoptosis* 2011;16:272–87.
- [4] Brault C, Levy PL, Bartosch B. Hepatitis C virus-induced mitochondrial dysfunctions. *Viruses* 2013;5:954–80.
- [5] Kaarbo M, Ager-Wick E, Osenbroch PO, Kilander A, Skinner R, Muller F, et al. Human cytomegalovirus infection increases mitochondrial biogenesis. *Mitochondrion* 2011;11:935–45.
- [6] Takahashi M, Wolf AM, Watari E, Norose Y, Ohta S, Takahashi H. Increased mitochondrial functions in human glioblastoma cells persistently infected with measles virus. *Antiviral Res* 2013;99:238–44.
- [7] Meylan E, Curran J, Hofmann K, Moradpour D, Binder M, Bartenschlager R, et al. Cardif is an adaptor protein in the RIG-I antiviral pathway and is targeted by hepatitis C virus. *Nature* 2005;437:1167–72.
- [8] Kawai T, Takahashi K, Sato S, Coban C, Kumar H, Kato H, et al. IPS-1, an adaptor triggering RIG-I- and Mda5-mediated type I interferon induction. *Nat Immunol* 2005;6:981–8.
- [9] Seth RB, Sun L, Ea CK, Chen ZJ. Identification and characterization of MAVS, a mitochondrial antiviral signaling protein that activates NF-kappaB and IRF 3. *Cell* 2005;122:669–82.
- [10] Hornung V, Ellegast J, Kim S, Brzozka K, Jung A, Kato H, et al. 5'-Triphosphate RNA is the ligand for RIG-I. *Science* 2006;314:994–7.
- [11] Schlee M, Roth A, Hornung V, Hagmann CA, Wimmenauer V, Barchet W, et al. Recognition of 5' triphosphate by RIG-I helicase requires short blunt double-stranded RNA as contained in panhandle of negative-strand virus. *Immunity* 2009;31:25–34.
- [12] Pichlmair A, Schulz O, Tan CP, Naslund TI, Liljestrom P, Weber F, et al. RIG-I-mediated antiviral responses to single-stranded RNA bearing 5'-phosphates. *Science* 2006;314:997–1001.
- [13] Kato H, Takeuchi O, Mikamo-Sato E, Hirai R, Kawai T, Matsushita K, et al. Length-dependent recognition of double-stranded ribonucleic acids by retinoic acid-inducible gene-I and melanoma differentiation-associated gene 5. *J Exp Med* 2008;205:1601–10.
- [14] Sadeq S, Al-Hashimi S, Cusack CM, Werner A. Endogenous double-stranded RNA. *Noncoding RNA* 2021;7:15.
- [15] Dhir A, Dhir S, Borowski LS, Jimenez L, Teitell M, Rotig A, et al. Mitochondrial double-stranded RNA triggers antiviral signalling in humans. *Nature* 2018;560:238–42.
- [16] Kim Y, Park J, Kim S, Kim M, Kang MG, Kwak C, et al. PKR senses nuclear and mitochondrial signals by interacting with endogenous double-stranded RNAs. *Mol Cell* 2018;71:1051–63.
- [17] Grochowska J, Czerwinski J, Borowski LS, Szczesny RJ. Mitochondrial RNA, a new trigger of the innate immune system. *Wiley Interdiscip Rev RNA* 2022;13:e1690.
- [18] Burke JM, Gilchrist AR, Sawyer SL, Parker R. RNase L limits host and viral protein synthesis via inhibition of mRNA export. *Sci Adv* 2021;7:eabh2479.
- [19] Pietras Z, Wojcik MA, Borowski LS, Szweczyk M, Kulinski TM, Cysewski D, et al. Controlling the mitochondrial antisense – role of the SUV3-PNPase complex and its co-factor GRSF1 in mitochondrial RNA surveillance. *Molec Cell Oncol* 2018;5:e1516452.
- [20] Leszczyniecka M, Su ZZ, Kang DC, Sarkar D, Fisher PB. Expression regulation and genomic organization of human polynucleotide phosphorylase, hPNPase(old-35), a type I interferon inducible early response gene. *Gene* 2003;316:143–56.
- [21] Gewartowski K, Tomecki R, Muchowski L, Dmochowska A, Dzwonek A, Malecki M, et al. Up-regulation of human PNPase mRNA by beta-interferon has no effect on protein level in melanoma cell lines. *Acta Biochim Pol* 2006;53:179–87.
- [22] Schonborn J, Oberstrass J, Breyel E, Tittgen J, Schumacher J, Lukacs N. Monoclonal-antibodies to double-stranded-RNA as probes of RNA structure in crude nucleic-acid extracts. *Nucleic Acids Res* 1991;19:2993–3000.
- [23] Zhu Y, Zhang M, Wang W, Qu S, Liu M, Rong W, et al. Polynucleotide phosphorylase protects against renal tubular injury via blocking mt-dsRNA-P-KR-eIF2alpha axis. *Nat Commun* 2023;14:1223.
- [24] Reikine S, Nguyen JB, Modis Y. Pattern recognition and signaling mechanisms of RIG-I and MDA5. *Front Immunol* 2014;5:342.
- [25] Wang DDH, Shu Z, Lieser SA, Chen PL, Lee WH. Human mitochondrial SUV3 and polynucleotide phosphorylase form a 330-kDa heteropentamer to cooperatively degrade double-stranded RNA with a 3' to 5' directionality. *J Biol Chem* 2009;284:20812–21.
- [26] Boye E, Grallert B. eIF2 alpha phosphorylation and the regulation of translation. *Curr Genet* 2020;66:293–7.
- [27] Wang ML, Cao RY, Zhang LK, Yang XL, Liu J, Xu MY, et al. Remdesivir and chloroquine effectively inhibit the recently emerged novel coronavirus (2019-nCoV) in vitro. *Cell Res* 2020;30:269–71.
- [28] Dong LY, Hu SS, Gao JJ. Discovering drugs to treat coronavirus disease 2019 (COVID-19). *Drug Discov Ther* 2020;14:58–60.
- [29] Zeng YM, Xu XL, He XQ, Tang SQ, Li Y, Huang YQ, et al. Comparative effectiveness and safety of ribavirin plus interferon-alpha, lopinavir/ritonavir plus interferon-alpha, and ribavirin plus lopinavir/ritonavir plus interferon-alpha in patients with mild to moderate novel coronavirus disease 2019: study protocol. *Chin Med J* 2020;133:1132–4.
- [30] Hoffmann M, Kleine-Weber H, Schroeder S, Kruger N, Herrler T, Erichsen S, et al. SARS-CoV-2 cell entry depends on ACE2 and TMPRSS2 and is blocked by a clinically proven protease inhibitor. *Cell* 2020;181:271.
- [31] Ou XY, Liu Y, Lei XB, Li P, Mi D, Ren LL, et al. Characterization of spike glycoprotein of SARS-CoV-2 on virus entry and its immune cross-reactivity with SARS-CoV. *Nat Commun* 2020;11:1620.
- [32] McArthur K, Whitehead LW, Heddleston JM, Li L, Padman BS, Oorschot V, et al. BAK/BAX macropores facilitate mitochondrial herniation and mtDNA eflux during apoptosis. *Science* 2018;359:883.
- [33] Sarkar D, Park ES, Fisher PB. Defining the mechanism by which IFN-beta downregulates c-myc expression in human melanoma cells: pivotal role for human polynucleotide phosphorylase (hPNPaseold-35). *Cell Death Differ* 2006;13:1541–53.
- [34] Tigano M, Vargas DC, Tremblay-Belzile S, Fu Y, Sfeir A. Nuclear sensing of breaks in mitochondrial DNA enhances immune surveillance. *Nature* 2021;591:477.
- [35] Sarkar D, Leszczyniecka M, Kang DC, Lebedeva IV, Valerie K, Dhar S, et al. Down-regulation of myc as a potential target for growth arrest induced by human polynucleotide phosphorylase (hPNPase(old-35)) in human melanoma cells. *J Biol Chem* 2003;278:24542–51.
- [36] Cheung YY, Chen KC, Chen HX, Seng EK, Chu JH. Antiviral activity of lanatoside C against dengue virus infection. *Antiviral Res* 2014;111:93–9.
- [37] Hoffmann HH, Palese P, Shaw ML. Modulation of influenza virus replication by alteration of sodium ion transport and protein kinase C activity. *Antiviral Res* 2008;80:124–34.
- [38] West AP, Khoury-Hanold W, Staron M, Tal MC, Pineda CM, Lang SM, et al. Mitochondrial DNA stress primes the antiviral innate immune response. *Nature* 2015;520:553–7.
- [39] Zhang C, Freddolino PL, Zhang Y. COFACTOR: improved protein function prediction by combining structure, sequence and protein-protein interaction information. *Nucleic Acids Res* 2017;45:W291–9.
- [40] Forli S, Huey R, Pique ME, Sanner MF, Goodsell DS, Olson AJ. Computational protein-ligand docking and virtual drug screening with the AutoDock suite. *Nat Protoc* 2016;11:905–19.
- [41] Yang Y, Yao K, Repasky MP, Leswing K, Abel R, Shoichet BK, et al. Efficient exploration of chemical space with docking and deep learning. *J Chem Theory Comput* 2021;17:7106–19.